Brightness and Polarization Distributions of Head-tail Galaxies at 1415 1~1iEIz

Miley, G.K.

Astron. & Astrophys. 26, 413 – 421 (1973)

Brightness and Polarization Distributions of Head-tail Galaxies at 1415 MHz

G. K. Miley
Sterrewacht, Leiden

February 22, 1973

Summary. Detailed 1415 MHz brightness and polarization distributions are presented for 3 C 129, NGC 1265 and IC 310 with a resolution of $\sim 23'' \times 30''$. For each of the sources the percentage polarization increases with distance from the optical galaxy. A comparison of these data with previous 408 MHz measurements gives useful spectral information. It is suggested that 3 C 129.1 is another example of a head-tail galaxy.

Key words: radio galaxies – clusters – polarization

1. Introduction

During the last few years observations carried out with the Cambridge One Mile Telescope have revealed the existence of a new class of relatively weak radio galaxies. These galaxies are characterized by a peculiar elongated radio morphology. The radio sources have a tadpole-like structure with a high brightness "head" close to the optical galaxy and a narrow low brightness "tail" extending for many minutes of arc.

There are now at least six radio galaxies of this type known and all appear to be associated with clusters of galaxies. Three are located in the Perseus Cluster (Ryle and Windram, 1968; Miley *et al.*, 1972) one is in the Coma Cluster (Willson, 1969) and a fifth is connected with the radio source 3 C 129 (Hill and Longair, 1971). Although 3 C 129 is in a very obscured region of the sky ($l = 160°$, $b = 0°$) Hill and Longair report that there are several other galaxies nearby and suggest that it is probably also situated in a cluster. A sixth example, PKS 2247 + 11, has recently been discovered in the cluster Zw 2247.3 + 1107 (Ekers and Schlizzi, private communications).

Two theories have been advanced to account for the existence of these "head-tail" radio galaxies. The first, the "interacting galaxies" hypothesis was proposed by Ryle and Windram chiefly to explain the geometrical configurations found in their radio observations of the Perseus Cluster. The galaxies NGC 1265 and IC 310 had radio tails which appeared to point roughly away from the nearby active galaxy NGC 1275 and this led Ryle and Windram to suggest that a wind of relativistic particles from NGC 1275 blows past the other two galaxies, igniting radio sources during the encounter. Although the suggested candidates for the igniting galaxies were less convincing in the Coma and 3 C 129 cases, Hill and Longair continued to support the interacting viewpoint. Using the Westerbork telescope Miley *et al.* (1972) recently discovered a third head-tail galaxy in the Perseus Cluster. Since here the tail appears to point almost toward NGC 1275, this detection further weakened the case for the interacting galaxies hypothesis.

Miley *et al.* proposed an alternative explanation. They suggested that the head-tail galaxies are radio sources in their own right independent of any external influence and that the radio tails are merely remnants left behind by the galaxies in their motion through the cluster. Additional arguments advanced in favour of this "radio trail" viewpoint were the high velocity dispersion of the Perseus Cluster and the double nature and high polarization of the radio tails as deduced from a preliminary analysis of the 1415 MHz Westerbork observations. Here we present the detailed brightness and polarization maps derived from these measurements for 3 C 129, NGC 1265 and IC 310 and compare our data with the Cambridge 408 MHz results.

2. Observing and Reduction Procedure

The Westerbork telescope (Baars and Hooghoudt, 1972; Casse and Muller, 1972) consists of twelve 25 m paraboloids along a 1.6 km east-west line. Ten of these are fixed and the remaining two can be moved along a 300 m railtrack. At the focus of each paraboloid is a pair of crossed dipoles which measure orthogonal components of the incoming wave. The two outputs of each movable dish are correlated with the two outputs of every fixed dish to provide simultaneous measurements of four different complex amplitudes from twenty separate interferometer baselines.

The use of the Westerbork telescope as a polarimeter has been described by Weiler (1973). Throughout all our measurements the telescope was used in the normal operating mode with the crossed dipoles on the movable dishes oriented at 45° with respect to those of the fixed dishes. For each baseline simple linear combinations of the four output channels give the complex fringe amplitudes corresponding to the four Stokes parameters I, Q, U and V. A Fourier transform of the fringe amplitude data then gives a map of the sky distribution of the relevant Stokes parameter over a region of the sky defined by the antenna pattern of a 25 m dish ($\sim 37'$ half power diameter) whose resolution is governed by the synthesized beam. This is the calculated response of the instrument to a point source and depends on the exact baseline coverage and grading function used. Each of the three galaxies was observed for a total of 4×12 hours thereby resulting in data from eighty contiguous baselines with lengths ranging from 36 to 1458 m in intervals of 18 m.

The standard Westerbork calibration procedure (Brouw, 1971) was used throughout the measurements and the calibrators 3 C 48 and 3 C 147 were observed regularly. Both are point sources with linear polarization less than $\sim 0.5\%$ at 21.2 cm (Morris and Berge, 1964; Bologna *et al.*, 1969) Westerbork observations give their relative polarization to be less than 0.5%. They were therefore assumed to be unpolarized with 1415 MHz flux densities of 15.67 and 21.57 flux units respectively.

For optimum compromise between high resolution and low sidelobe level a Gaussian grading function was applied to the visibility data before transformation. This taper gives progressively less weight to the longer baselines and varied from unity, to 0.25 at the longest baseline. The resulting synthesized beam is elliptical with half-power diameters $22''$ in right ascension by $22'' \operatorname{cosec}\delta$ in declination and the *rms* noise on the map is equivalent to $\sim 0.6 \times 10^{-29}$ W m^{-2} H$_z^{-1}$. In addition it was found useful to use a steeper grading function to produce a map whose synthesized beam is about three times larger. In both cases the first diffraction grating ring is located $40'$ in right ascension and $40' \operatorname{cosec}\delta$ in declination from the centre of the synthesized beam.

The maximum scale of structure that can be observed with the instrument depends on the shortest interferometer spacing used. When observed with the 36 m spacing a Gaussian source of $5'$ extent would have a visibility of $\sim 80\%$. Thus structures with scales much larger than $5'$ will be severely attenuated.

The lack of information from the zero and 18 m spacings also changes the zero level on the map. The missing zero spacing introduces a constant offset whereas the missing 18 m spacing produces a variable offset with a period $\sim 40' \times 40' \operatorname{cosec}\delta$. The magnitude of both these effects depends on the strength and distribution of brightness in the field.

The interferometers of a synthesis instrument measure intensities corresponding to the appropriate spatial frequencies and they are calibrated using point sources of known flux density. The Fourier transforms then give maps of the four Stokes parameters which are expressed in units of flux density, where the indicated flux density at a point on the map is the strength of an unresolved source which would give the same brightness if located at that point. To convert to units of brightness such as brightness temperature one must first divide the flux densities on the map by the solid angle of the synthesized beam. Since the beam does not have well defined boundaries and since the smaller spacing data is missing, this conversion process is not accurately specifiable. Moreover the brightness temperatures so derived are lower limits that would increase if higher resolution observations should reveal clumpiness. It has therefore been decided that the maps are most usefully described in the original units of flux density per synthesized beam area. However, for structure in the range of spatial frequencies observed, conversion from flux density S in mfu to brightness temperature T in K for a source at a declination δ, is given to an accuracy of $\sim 5\%$ by the formula $T = 1.21\, S \sin\delta$. For the polarization maps the temperatures thus derived lie on the "BHS" scale (Berkhuijsen *et al.*, 1973). To convert to the "WSBT" scale (Westerhout *et al.*, 1962) they must be multiplied by a factor of two.

3. Presentation of the Results

a) The Contour Maps

For each source we present two contour maps of the total intensity I. The first is designed to show the broad features of the brightness distribution and the second gives a more detailed picture of the low brightness features in the tail. In both cases continuous contours are plotted at 5% intervals from zero to the indicated value of I. MAX, and these are supplemented by long dashed contours representing the 2.5% level and short dashed contours the -2.5% and -5% levels. A cross marks the optical position of the galaxy. In these contour maps no account has been taken of the variation in map zero level due to the missing 18 m spacing. This effect is about 4 mfu for 3 C 129, 2 mfu for NGC 1265 and is negligible for IC 310.

Also given for each source is a contour map of the linearly polarized intensity $P = (Q^2 + U^2)^{\frac{1}{2}}$ with the polarization position angles $\phi = \frac{1}{2}\,\mathrm{tg}^{-1}(U/Q)$ indicated on it. These contours are plotted at 10% intervals from zero to the indicated value of P. MAX.

All the contour maps are uncorrected for attenuation by the $36'$ primary beam but the positions of the beam centre are shown. The sharp appearance of the contours

Table 1. Comparison of the grading functions used in the different maps

	1415 MHz	1415 MHz convolved	408 MHz
Shortest spacing	170 λ	255 λ	256 λ (3 C 129)
	170 λ	170 λ	128 λ (NGC 1265, IC 310)
Baseline increment	85 λ	255 λ	256 λ (3 C 129)
	85 λ	170 λ	128 λ (NGC 1265, IC 310)
Longest spacing	6881 λ	2019 λ	2044 λ
gaussian taper	25% at 6881 λ	30% at 2044 λ	30% at 2044 λ

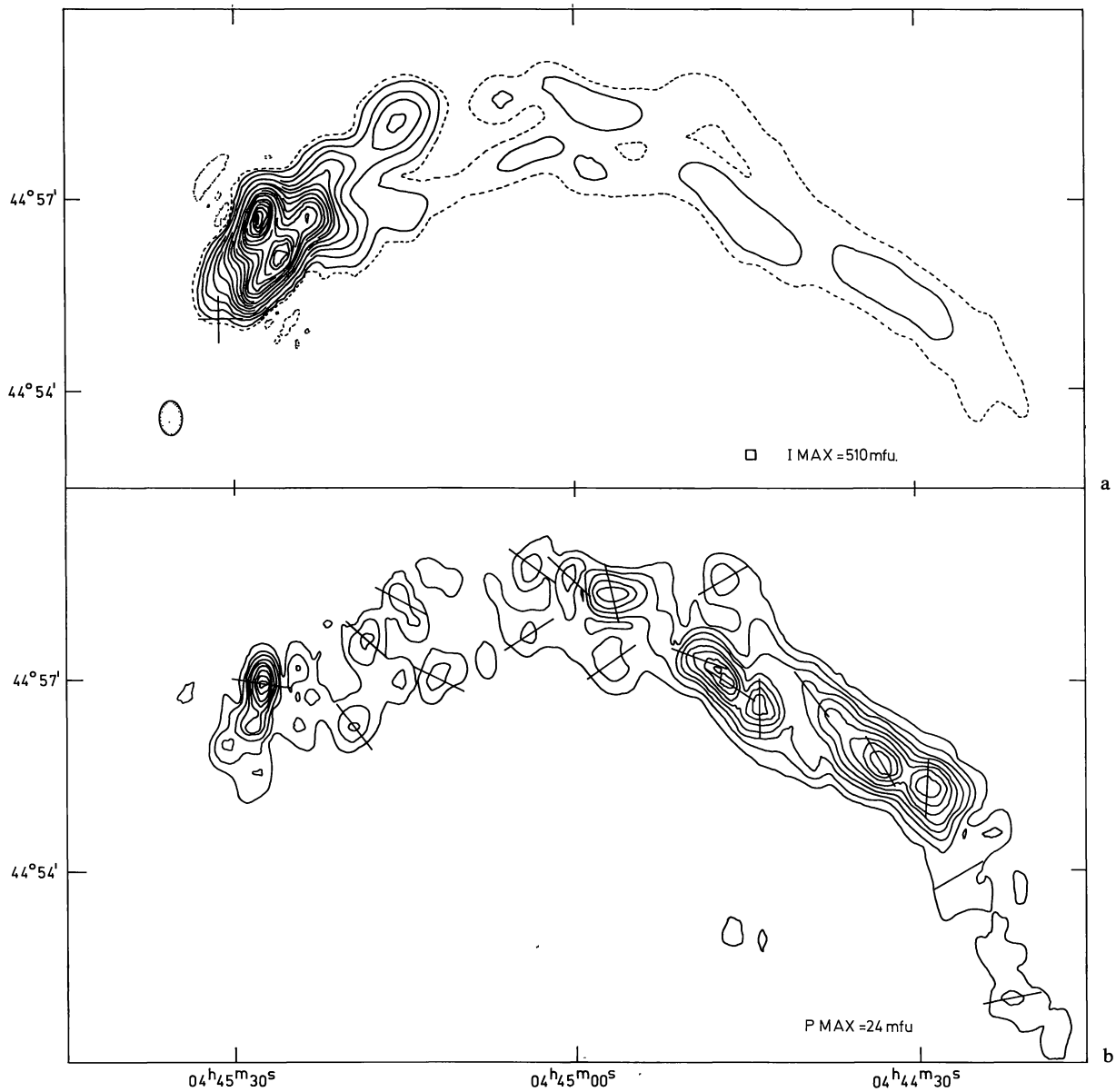

Fig. 1a. The total intensity distribution of 3 C 129. Continuous contours are plotted at 5% intervals from zero to the indicated value of I.MAX. Long dashed contours represent the 2.5% level and short dashed contours the −2.5% and −5% levels. The cross shows the optical position of galaxy, the ellipse indicates the half-power contour of the synthesized beam and the square gives the centre of the primary beam
Fig. 1b. The polarization distributions of 3 C 129. Continuous contours are plotted at 10% intervals from zero to the indicated value of P.MAX

is due to the contour plotting method which interpolates linearly between the grid points on the map; these are never closer than a third of a synthesized beamwidth.

b) Variation of Brightness along the Tails

To obtain the variation of brightness with distance along the tails the maps were convolved to a resolution lower by a factor of three. The flux densities were estimated from intensity profiles taken through the tails at the appropriate points thus minimising the effects of the changing zero level due to the missing data at the 18 m spacing. These data are corrected for attenuation by the primary beam.

c) The Width of the Tails

Two parameters have been used to characterise the width of the tails, $\theta_{\frac{1}{2}}$ the largest width to half intensity and $\theta_{\frac{1}{4}}$ the largest width to a quarter intensity. Dissimilar behaviour of $\theta_{\frac{1}{2}}$ and $\theta_{\frac{1}{4}}$ indicates that one side of tail is brighter than the other.

d) Comparison of the 1415 and 408 MHz Observations

To derive spectral information on the head-tail sources, convolved 1415 MHz maps were produced whose synthesized beams resembled as closely as possible those used in the Cambridge 408 MHz observations. The relevant parameters are shown in Table 1. The 408 MHz data was kindly supplied in quantitative form by Mrs. Julia Riley (née Hill). For both frequencies, effects due to the absence of short spacing data were minimised by obtaining the flux densities from intensity profiles through the tails at the same positions in similar directions. Also the 1415 MHz data were corrected for attenuation by the narrower primary beam.

e) The Percentage Polarizations

We give a graph of the variation of percentage polarizations with distance along the tail. The percentage polarizations were also estimated from intensity profiles, taken at the same points on the total intensity and polarization maps to minimise effects

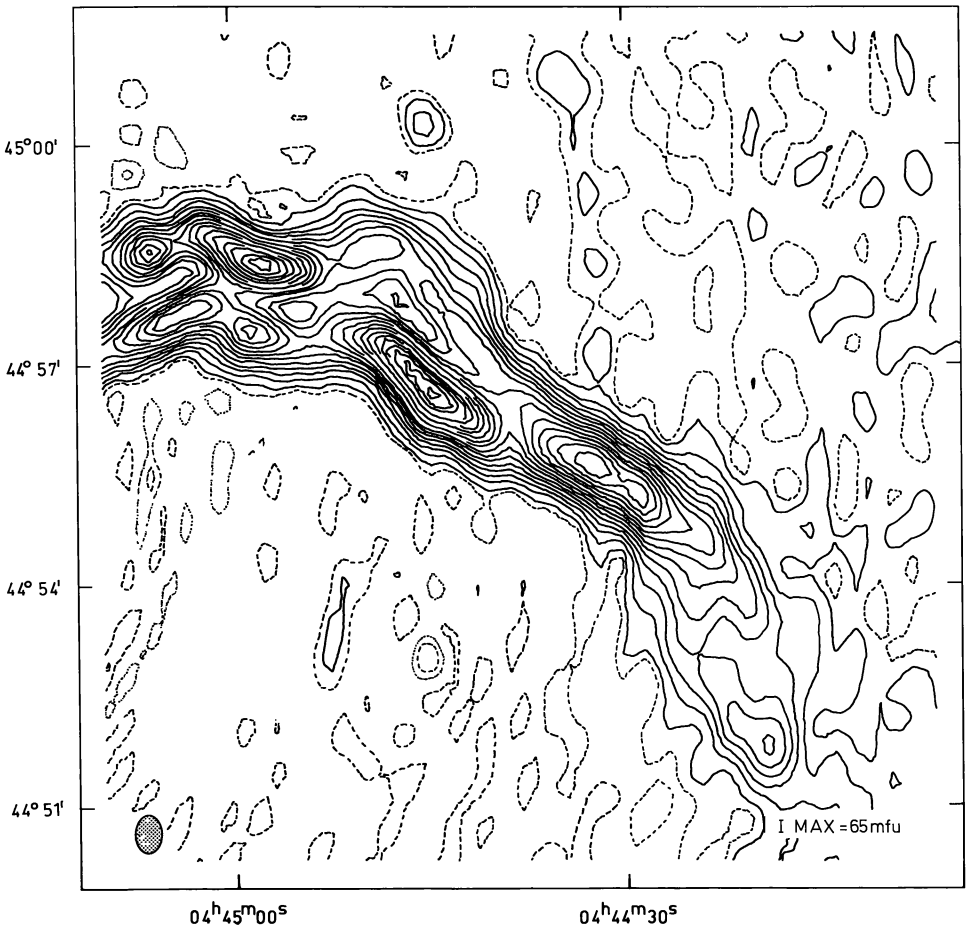

Fig. 2. The total intensity distribution of the 3 C 129 tail. Contours are plotted at the same levels as described for Fig. 1a relative to the new indicated I.MAX. All coordinates in this article are 1950 ones

due to the missing spacings. In regions where the tails are clearly double we show percentage polarizations for both components.

4. Errors

The I, Q, U and V maps are all subject to the following errors: (1) random noise ~ 0.8 mfu rms (2) calibration errors $\sim 5\%$ (3) sidelobe distortion $\sim 5\%$ close to the brightest peaks (4) distortion of the map and its zero level due to the missing zero and 18 m spacings (see above). In addition the Q, U and V maps are subject to instrumental uncertainties whose magnitude are $\sim 5\%$ of I. At no point on any of the V-maps was V found to be larger than 5% of the maximum value of I. No circular polarization is expected and its absence to this level is a partial check on the estimated errors in Q and U.

The polarized intensities $(P=(Q^2+U^2)^{\frac{1}{2}})$ position angles $(\phi=\frac{1}{2}\,\mathrm{tg}^{-1}(U/Q))$ and percentages $(m=100P/I)$ are all non linear combinations of observable quantities and the errors, particularly for ϕ and m, are difficult to estimate. Near the radio heads where sidelobe distortion predominates it is believed that the errors in the position angles shown are $\sim \pm 10°$ and in percentages $\sim \pm 20\%$ of the quoted values. At other positions in the tails the corresponding errors are $\sim \pm 5°$ and $\sim \pm 10\%$ respectively.

5. Results and Discussion

a) 3 C 129

The results for 3 C 129 are shown in Fig. 1–3. Following Hill and Longair a distance of 50 Mpc has been assumed in calculating linear scales. 3 C 129 is a truly remarkable source. Its tail extends for nearly 400 kpc and is therefore one of the largest known radio galaxies. Note the double nature of both the head and the tail. The tail is not smooth but has a clumpy appearance with individual blobs having flux densities of between 0.05 and $0.7\times10^{-26}\,\mathrm{W\,m^{-2}\,Hz^{-1}}$ corresponding to 1415 MHz luminosities of $\sim 1.5\times10^{22}$ to $2\times10^{23}\,\mathrm{W\,Hz^{-1}}$ respectively. The radio spectrum steepens and the linear polarization increases fairly steadily along the tail

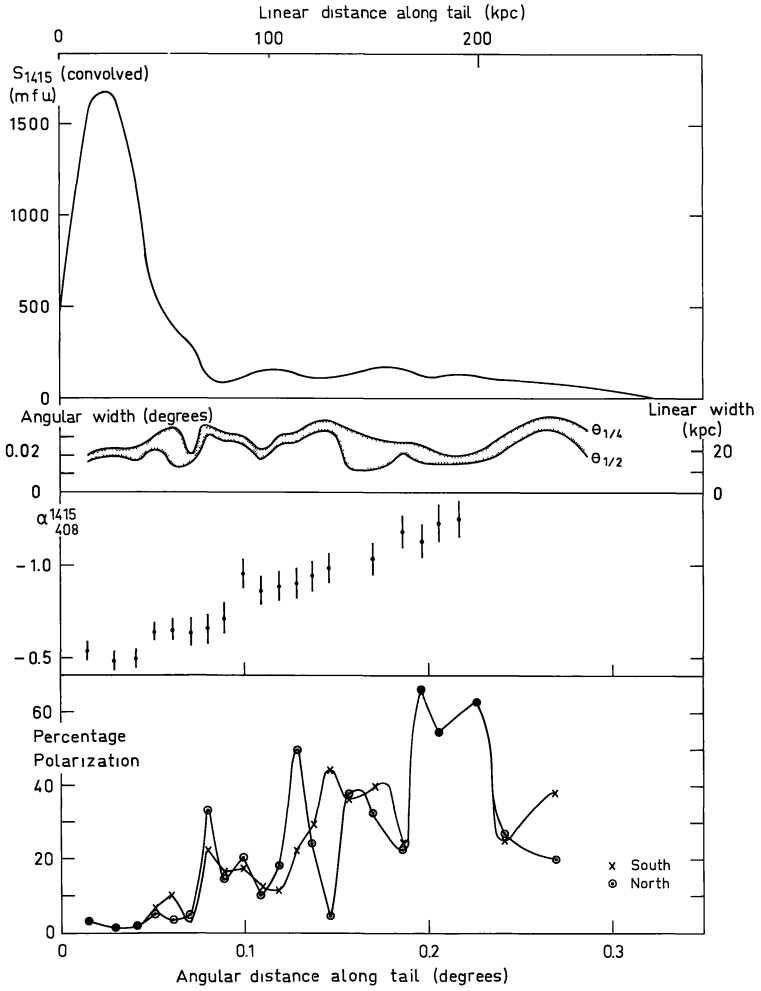

Fig. 3. Variation of brightness, width, spectral index and percentage polarization along the tail of 3 C 129. (Assumed distance 50 Mpc)

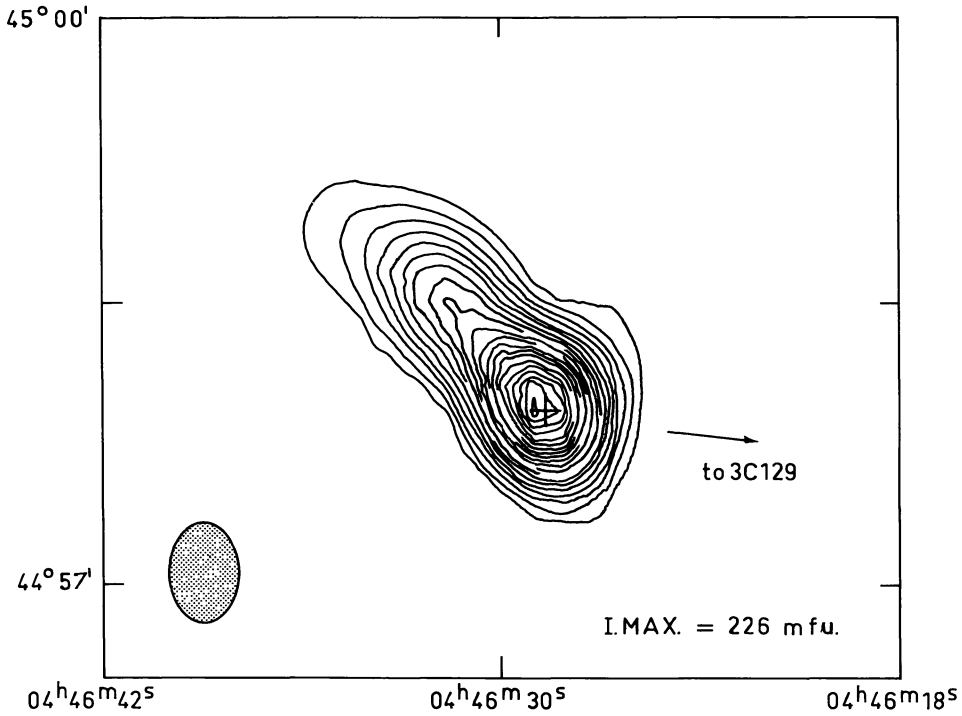

Fig. 4. The total intensity distribution of 3 C 129.1. Contours are plotted at the same levels as described for Fig. 1a relative to the new indicated I.MAX. The cross shows the optical positions of the galaxy

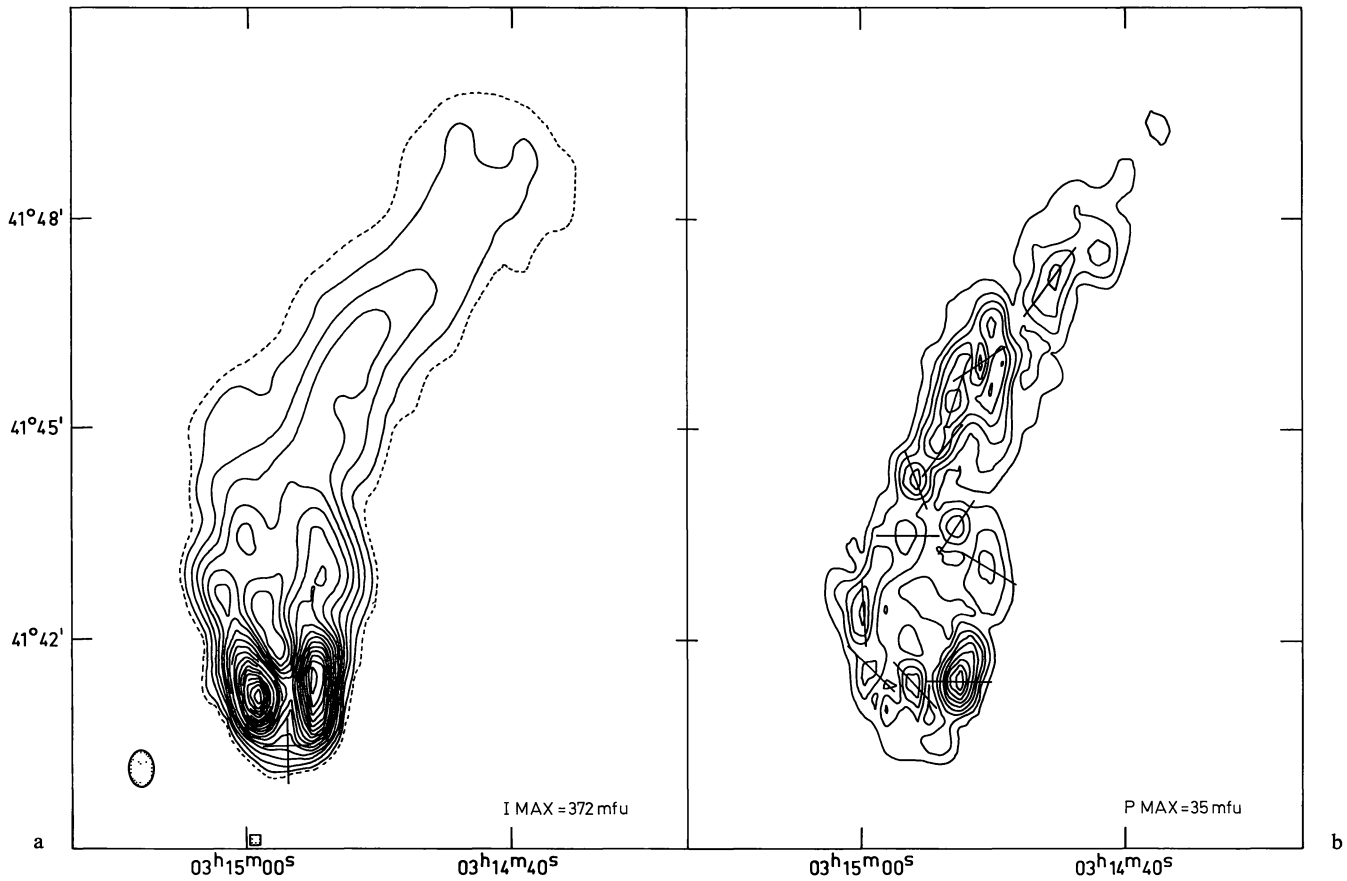

Fig. 5a. The total intensity distributions of NGC 1265. Contours are plotted at the same levels as described for Fig. 1a relative to the new indicated I.MAX

Fig. 5b. The polarization distribution for NGC 1265. Contours are plotted at 10% intervals from zero to the indicated value of P.MAX

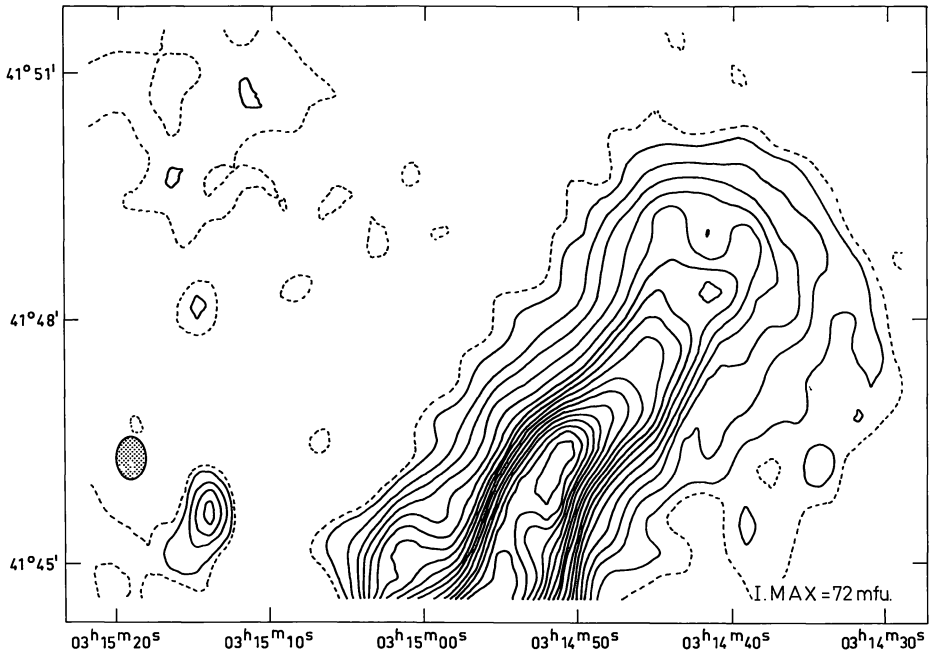

Fig. 6. The total intensity distribution of the NGC 1265 tail. Contours are plotted at the same levels as described for Fig. 1a relative to the new indicated I.MAX

indicating that the further the region of radio emission from the galaxy the older and more ordered it is. The peak degree of linear polarization (about 60%) is one of the largest known for any radio source and occurs at the point where the tail narrows. This apparent constriction in the tail, also visible on the radio photograph, was interpreted by Miley *et al.*, as indicating that the radio ejection axis of the galaxy may rotate as it traverses the cluster.

b) 3 C 129.1

Figure 4 shows a contour map of the brightness distribution of 3 C 129.1, the source associated with the galaxy thought by Hill and Longair to be the cause of the 3 C 129 radio emission. However, its radio power is less than a twentieth of that of NGC 1275, the suggested ignition galaxy in the Perseus Cluster and the radio morphologies of 3 C 129.1 and NGC 1275 are very different. The position of the optical galaxy (marked by the cross in Fig. 2) suggests that 3 C 129.1 is simply another example of a "head-tail" galaxy.

c) NGC 1265

The results for NGC 1265 are shown in Figs. 5–7. Like 3 C 129 this galaxy also has a double head, a double tail and a polarization percentage which increases with distance along the tail. There are however several significant differences. Firstly, the brightness in the tail of NGC 1265 is distributed more continuously and does not have the clumpy appearance seen in 3 C 129.

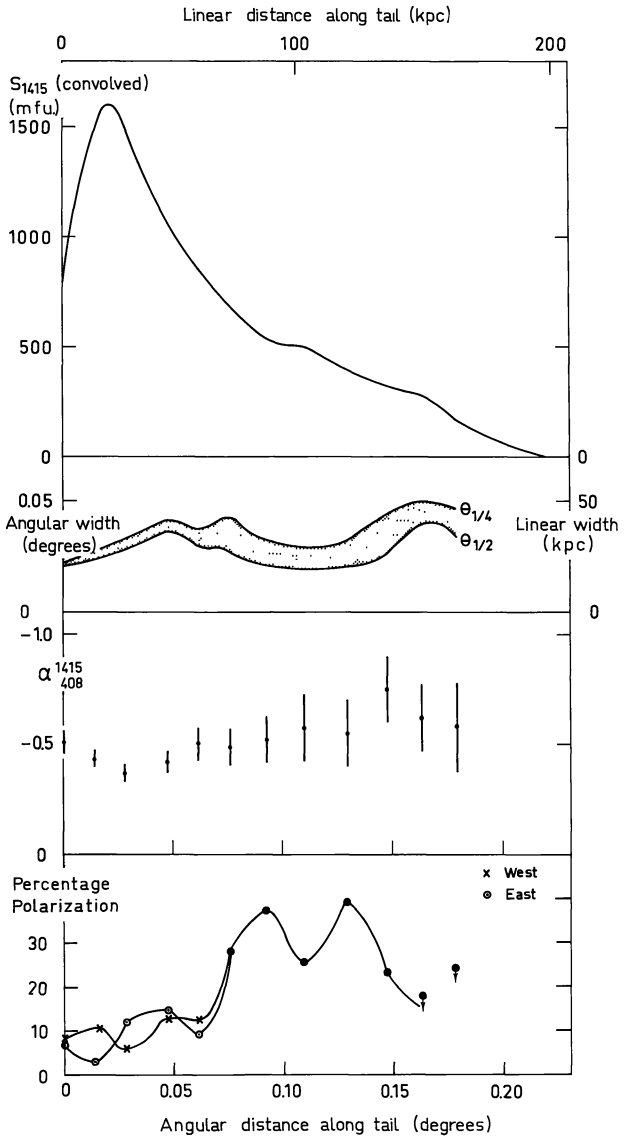

Fig. 7. Variation of brightness, width, spectral index and percentage polarization along the tail of NGC 1265. (Assumed distance 60 Mpc)

Secondly the change in brightness between head and tail occurs much more gradually than in 3 C 129. Thirdly, there is not such a marked increase in spectral index. Fourthly, the tail ends abruptly rather than trailing into the noise as is the case for 3 C 129. Projection effects within the "ploughing galaxy" model, could produce some but not all of the differences observed. Since the radial velocity of NGC 1265 is 2300 km^{-1} different from that of the mean of the Perseus Cluster (Chincarini and Rood, 1971), this galaxy is probably moving in a direction almost towards us. If one imagines observing 3 C 129 from a

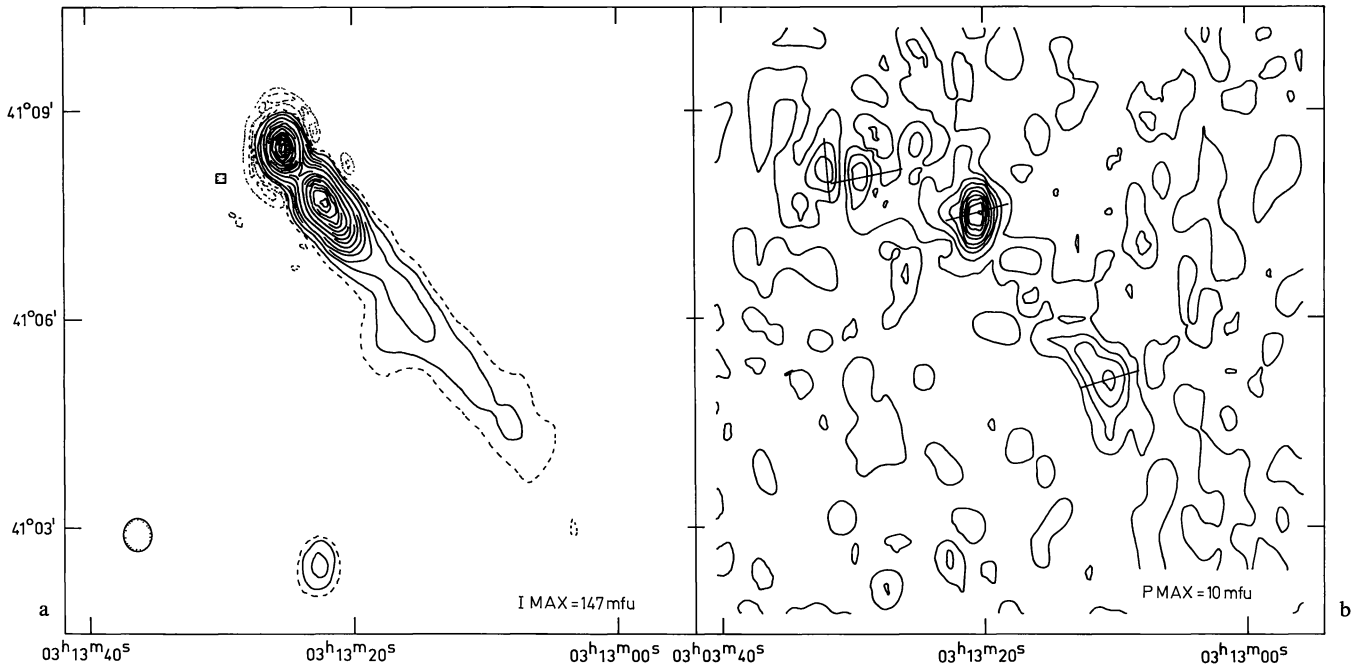

Fig. 8a. The total intensity distribution of IC 310. Contours are plotted at the same levels as described for Fig. 1 relative to the new indicated I.MAX. The cross shows the positions of the optical galaxy
Fig. 8b. The polarization distribution of the IC 310 tail. Contours are plotted at 10% intervals from zero to the indicated value of P.MAX

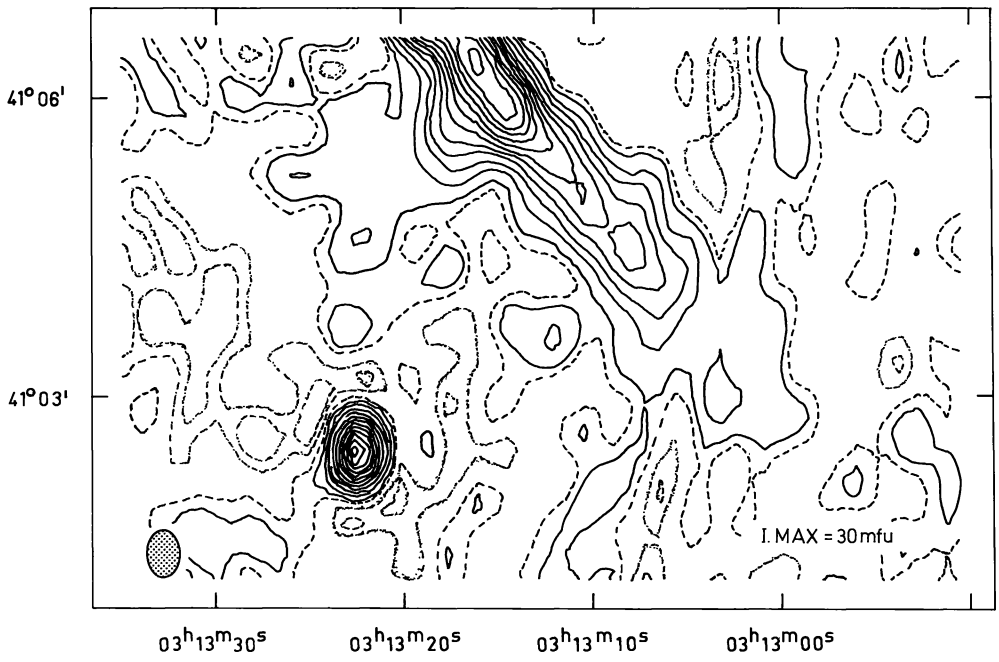

Fig. 9. The total intensity distributions of the IC 310 tail. Contours are plotted at the same levels as described for Fig. 1 relative to the new indicated I.MAX

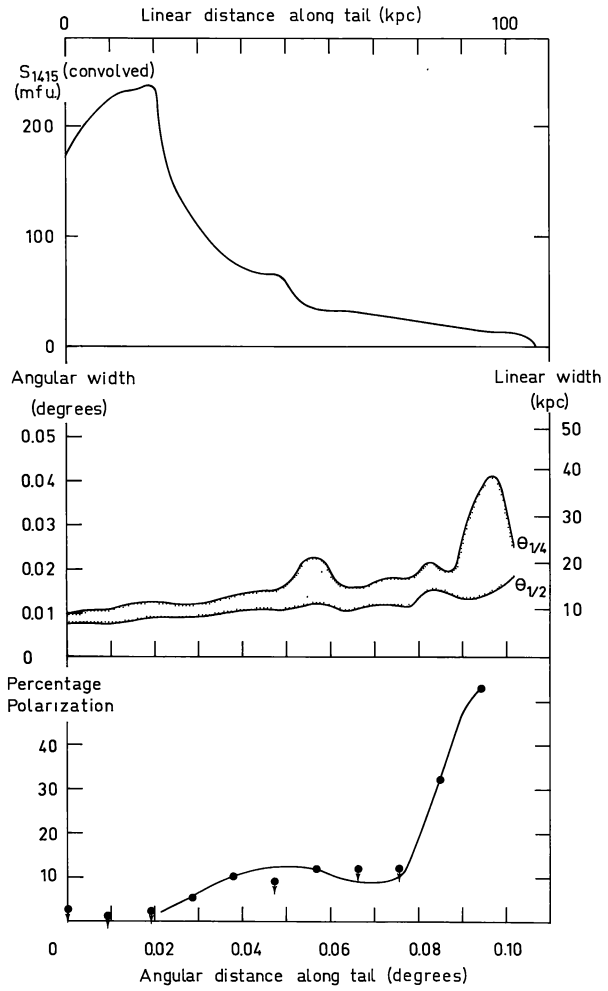

Fig. 10. Variations of brightness, width and percentage polarization along the tail of IC 310. (Assumed distance 60 Mpc)

position almost in front of it, the contributions from different points along the tail would add and the brightness distribution would appear more continuous.

d) IC 310

For IC 310 no 408 MHz data was available and so it was not possible to derive spectral information. The results are presented in Figs. 8–10 and it is clear that for this source also the percentage polarization increases along the tail. The tail of IC 310 appears remarkably straight and narrow when compared with those of NGC 1265 and 3 C 129. Because the radio luminosity of IC 310 is lower than that of NGC 1265 by a factor of ~ 10 it is quite conceivable that the radio plasmoids were ejected with less kinetic energy and therefore would not travel as far before being stopped by ram pressure forces. Measurements with higher resolution may reveal that the IC 310 head-tail also has a double structure.

A weak (~ 20 mfu) source lies close to a bulge in the IC 310 tail. It is interesting to note from Fig. 6 a similar coincidence in the case of NGC 1265. Both sources may be causally unrelated to the head-tail galaxies or alternatively they could be plasmoids which have "escaped" from unstable regions of the tails.

6. Conclusion

We have suggested how the similarities and differences between the head-tail galaxies can be understood in terms of the radio trail model. Detailed model calculations will be presented by Jaffe and Perola in a subsequent paper. Further observations of these objects are planned using the Westerbork telescope at 0.6 and 5.0 GHz. The resulting spectral and polarization data should give much useful information on the physical parameters of the sources and on the conditions within clusters. A knowledge of the distribution of magnetic fields and plasma densities will narrow the range of possible models.

Acknowledgements. I thank Mrs. Julia Riley for providing the Cambridge 408 MHz data in quantitative form. The Westerbork Radio Observatory is operated by the Netherlands Foundation for Radio Astronomy with the financial support of the Netherlands Organization for the Advancement of Pure Research (Z.W.O.).

References

Baars, J. W. M., Hooghoudt, B. 1972, *Astron. & Astrophys.* in press.
Berkhuijsen, E. M., van de Hulst, H. C., Spelstra, T. A. 1973, in preparation.
Bologna, J. M., McClain, E. F., Sloanaker, R. M. 1969, *Astrophys. J.* **139**, 248.
Casse, J., Muller, L. 1972, *Astron. & Astrophys.*, in press.
Chincarini, G., Rood, H. J. 1971, *Astrophys. J.* **168**, 321.
Hill, J. M., Longair, M. S. 1971, *Monthly Notices Roy. Astron. Soc.* **154**, 125.
Miley, G. K., Perola, G. C., van der Kruit, P. C., van der Laan, H. 1972, *Nature* **237**, 269.
Morris, D., Berge, G. L. 1964, *Astron. J.* **69**, 641.
Ryle, M., Windram, M. D. 1968, *Monthly Notices Roy. Astron. Soc.* **138**, 1.
Weiler, K. 1973, *Astron. & Astrophys.*, in press.
Westerhout, G., Seeger, C., Brouw, W. N., Tinbergen, J. 1962, *Bull. Astron. Inst. Neth.* **16**, 187.
Willson, M. A. G. 1970, *Monthly Notices Roy. Astron. Soc.* **151**, 1.

G. K. Miley
Sterrewacht
Leiden 2401, The Netherlands